SKILLING, HELLE, CHRISTIANSEN, ROBERTSON
Consulting Structural & Civil Engineers
345 Park Avenue, New York, N. Y. 10017

TRANSMITTAL LETTER

Date July 8. 1968

To: Laclede Steel Company
Arcade Building
St. Louis, Missouri 63101

Subject:

Attn:

Gentlemen: We are transmitting herewith the following:

☐ **Drawings as listed below**

☐

This material is sent: ☐ **By your request** ☐ **For your use or information**

☐ **For your comment** ☐

Drawing No.	No. of copies	Date	Description
			We are returning Interpretation of Composite Joist Test Results by T. V. Galambos and R. Tide. Thank you for its use.

Remarks:

SKILLING, HELLE, CHRISTIANSEN, ROBERTSON

by: James White

James White

Transmitted Via:
☐ Messenger
☐ 1st Class Mail
☐ Air Mail
☐ Special Delivery
☐ Air Express

Transmittal Copy.

RECEIVED
OCT 19 1967
SKILLING · HELLE
CHRISTIANSEN · ROBERTSON
230 PARK AVE. N.Y.C.

COMPOSITE JOIST PROJECT

SPONSORED BY STEEL JOIST INSTITUTE

AT WASHINGTON UNIVERSITY, ST. LOUIS.

INTERPRETATION OF COMPOSITE JOIST TEST RESULTS

by T. V. Galambos and

R. Tide

September 1967

1. Types of Tests

Two types of structural tests were performed:

1) Cantilever tests (Fig. 1)

2) Beam tests (Fig. 2)

In each test deflection readings, slip readings at each shear connection location and strain readings were recorded for each load increment. The location of each gage is shown in Figs.3 for each test, and all recorded data are tabulated in the Appendix.

2. Load-Deflection Curves

The experimental load deflection curves are recorded in Figs. 4, grouped into tests with similar joists. Also shown in these figures are theoretical curves based on the assumption of (1) zero interaction and (2) complete interaction.

The theoretical deflection was computed in the following manner:

Beam tests, deflection at the center of the beam

$$\Delta = \frac{Pa}{24EI} (3L^2 - 4a^2) \qquad (1)$$

Cantilever tests, deflection at the free end

$$\Delta = \frac{Pa^3}{3EI} \tag{2}$$

For zero interaction the value of I used is $0.85I_s$, where I_s is the moment of inertia of the combined section consisting of the top and bottom chords. The 15% reduction is an arbitrary reduction to account for the effects of shear deformation, as is customary for joists.

For complete interaction the value of I was computed by assuming a modular ratio n = 9 and a reduced value of $0.85I_s$ was used for the steel section. The formulas for computing the I-s are given in Fig. 5 and their values are tabulated in Table 1.

The values of the shear span (a) for the cantilever tests were based on the distance from the load point to the point of apparent cantilever rotation. This occurred as a result of having the heavy tension chord connections.

The geometric arrangement in Fig. 5 is representative of both the cantilever and beam tests. The dimensioned variables are general enough so that they can represent the hot rolled, cold rolled, and extended web members of the test series.

The maximum theoretical load for zero interaction was determined from the assumption that failure occurred when the top chord would buckle.

$$P_o = \frac{A_{sT}\, F_{cr}\, de}{a} \tag{3}$$

The value of F_{cr} is determined from the assumption that in a standard non-composite joist the compression chord is designed to buckle at approximately the same time as the smaller tension chord yields.

The maximum theoretical load for complete interaction was determined from the assumption that failure occurred when the bottom chord yielded:

$$P_c = \frac{A_{sB} F_y \bar{y}_R}{s} \qquad (4)$$

3. Theoretical Analysis of Incomplete Interaction

3.1 Degree of interaction

For complete interaction there should be no slip between slab and joist. For zero interaction the slab and the joist should act independently, with the slab sliding over the beam without friction.

Amount of force carried by slab is determined by assuming that slab and joist deflect the same amount.

$$\Delta = \frac{P_s a}{24E_s I_s}\left(3L^2 - 4a^2\right) = \frac{P_c a}{24E_c I_c}\left(3L^2 - 4a^2\right)$$

from which

$$P_c = \frac{P_s E_c I_c}{E_s I_s} = \frac{P_s I_c}{nI_s} = \frac{27}{9I_s} = \frac{3P_s}{I_s}$$

For example, for B-1, 2, 4, 5, 6, $I_{sE} \approx 90$ in^2

$$\therefore P_c = \frac{P_s}{30}$$

Thus the slab could carry at most 3 to 4% of the total shear. The end slope for the beam tests is

$$\theta = \frac{Pa}{2EI}\left(L-a\right)$$

For beam tests B-1, 2, 4, 5, 6,

$$P_s \cong 0.97P, \quad L = 186 \text{ in}, \; a = 81 \text{ in}, \; E = 29{,}000 \text{ Ksi}, \; I_{sE} = 90 \text{ in}^9$$

$$\therefore \quad \theta \cong 16P \times 10^{-3} \text{ radians}$$

The slip $\Delta_s = \theta \left(d_e + d_g - \bar{y}_s + \frac{t}{2} \right)$

With $d_e = 15.2$ in, $d_g + \frac{t}{2} = 1.9$ in, $\bar{y}_s = 6.4$ in,
the end slip for tests B-1, 2, and 6 is

$$\Delta_s \cong 0.017P$$

It turns out that Δ_s for the other beam tests is nearly the same. The measured end slip for all the beam tests is compared to this fictitious maximum possible slip in Fig. 6. The curves lie between zero interaction and full interaction ($\Delta_s = o$ for any P).

Tests B3 and B4 (extended webs) are nearly fully composite.

The others are all partially composite, with decreasing degree of interaction as follows:

B6 - Two shear connectors at mid panel, two-angle chord

B2 - One shear connector at mid panel, two-angle chord

B1 - One shear connector at panel point, two-angle chord

B4 - One shear connector at mid panel, c.f. chord

B5 - One shear connector at panel point, c.f. chord

Thus shear connection was improved by shorter connectors, (B2 vs. B4, B1 vs.B5), by placing them at mid panel (B2 vs. B1, B4 vs. B5), and by increasing their size (B6 vs. B2)

Similar results can be seen for the cantilever tests in Fig. 7.

3.2 Assumptions

1) Elastic beam theory (as contrasted to truss theory)

2) Usefulness is terminated at first yield.

3) Strain distribution across section is linear.

4) Curvature of slab and joist is equal.

5) Bending in top chord angles is negligible.

6) Shear connection between joist and slab is continuous.

7) Change in slip is proportional to change in connecting shear force.

3.3 Analysis of Shear Connector Forces.

The forces and strains are shown in Fig. 8. Forces are shown as incremental forces; we assume that spring constant is the same during each load increment.

Equilibrium equations:

$$\delta N_c + \delta N_{ST} - \delta N_{SB} = 0 \tag{5}$$

$$\delta N_{SB}\, d_e + 1.9\delta N_c + \delta M_c = \delta M_x \tag{6}$$

Compatibility equations: (curvatures are equal).

$$\varphi = \frac{\delta M_c}{E_c I_c} = \frac{1}{d_e}\left(\frac{\delta N_{ST}}{A_{ST}\, E_S} + \frac{\delta N_{SB}}{A_{SB}\, E_S}\right)$$

or

$$\frac{\delta N_{ST}}{A_{ST}} + \frac{\delta N_{SB}}{A_{SB}} = \frac{n d_e\, \delta M_c}{I_c} \tag{7}$$

At level of c.g. of compression chord:

$$\frac{\delta N_c}{A_c E_c} - \frac{1.9\delta M_c}{I_c\, E_c} + \xi = \frac{\delta N_{ST}}{A_{ST}\, E_s} \tag{8}$$

Where ξ is discontinuity of strain = change in slip.

Δ_s = slip, + when in opposite direction to ξ

$\delta\Delta_s$ = change in slip for change in load δP

$$\therefore \quad \xi = - \frac{d\delta\Delta_s}{dx} \tag{9}$$

Where x is measured from end of member

Also

$$\Delta_s = \frac{D_o}{K} \tag{10}$$

Where D_o = Average connector force per unit length

K = Spring constant of continuous shear connection

Also $$D_o = \frac{dN_c}{dx} \tag{11}$$

Thus $$\delta\Delta_s = \frac{1}{K}\left(\frac{d\delta N_c}{dx}\right) \tag{12}$$

and $$\xi = - \frac{1}{K}\left(\frac{d^2\delta N_c}{dx^2}\right) \tag{13}$$

Setting Eq. 13 into Eq. 8 and eliminating δM_c, δN_{ST} and δN_{SB} from Eqs. 5, 6, 7 and 8, we get, after some algebra:

$$\delta N_c'' - C_A K \delta N_c = - C_B K \delta M_x \tag{14}$$

where $$\delta N_c'' = \frac{d^2\delta N_c}{dx^2}$$

$$C_A = \frac{1}{A_c E_c} + \frac{1.9 d_e}{I_c E_c}\left(\frac{\beta + \frac{1.9\beta}{de} + \frac{1.9}{de}}{}\right) + \frac{1}{E_s A_{ST}}\left(\frac{\alpha + 1 + \frac{1.9\alpha}{de}}{}\right) \tag{15}$$

$$C_B = \frac{1.9}{I_c E_c}\left(\frac{\beta + 1}{\alpha + \beta + 1}\right) + \frac{\alpha}{d_e E_s A_{ST} (\alpha+\beta+1)} \tag{16}$$

$$\alpha = \frac{nd_e^{\,2} A_{SB}}{I_c} \tag{17}$$

$$\beta = \frac{A_{SB}}{A_{ST}} \tag{18}$$

C_A & C_B are constants for any given specimen

The solution of eq. 14 is:

Shear span: $\delta M_x = \delta P_x$ $\qquad (o \leq x \leq a)$

$$\delta N_c = C_1 \sinh \gamma x + C_2 \cosh \gamma x + \frac{C_B \delta P X}{C_A} \tag{19}$$

Uniform moment region: $\delta M_x = \delta P a$ $\qquad (a \leq x \leq \frac{L}{2})$

$$\delta N_c = C_3 \sinh \gamma x + C_4 \cosh \gamma x + \frac{C_B \delta P a}{C_A} \tag{20}$$

where $\gamma = \sqrt{C_A K}$ (21)

Boundary Conditions:

$X = 0$ $\quad \delta N_c = 0$ $\quad$ No force in slab

$X = \frac{L}{2}$ $\quad \frac{d\delta N_c}{dx} = 0$ $\quad$ No slip

$X = a$ $\quad \delta N_c \text{ (Left)} = \delta N_c \text{ (Right)}$

$x = a$ $\quad \frac{d\delta N_c}{dx \text{ (Left)}} = \frac{d\delta N_c}{dx \text{ (Right)}}$

Upon substitution of these boundary conditions into Eqs. 19 & 20 we get:

$$\delta N_c = \frac{C_B \delta P}{C_A} \left[x - \frac{\sinh \gamma x}{\gamma} \left(\cosh \gamma a - \tanh \frac{\gamma L}{2} \sinh \gamma a \right) \right] \tag{22}$$

and

$$\frac{d(\delta N_c)}{dx} = \frac{C_B \delta P}{C_A}\left[1 - \cosh \gamma x \left(\cosh \gamma a - \tanh \frac{\gamma L}{2} \sinh \gamma a\right)\right] \quad (23)$$

Eq. 23 holds for the beam tests.

For the cantilever tests $\frac{L}{2} = a$ and so

$$\frac{d(\delta N_c)}{dx} = \frac{C_B \delta P}{C_A}\left[1 - \frac{\cosh \gamma x}{\cosh \gamma a}\right] \quad (24)$$

Eqs. 23 or 24 form the basis of determining the shear connector Force - Slip curve. We proceed as follows:

From Eq. 12, the change in slip is defined as

$$\delta \Delta_s = \frac{1}{K}\left(\frac{d\delta N_c}{dx}\right)$$

Introducting a function:

$$G(k) = G = 1 - \cosh \sqrt{C_A K'} \times \left(\cosh \sqrt{C_A K} a - \tanh \sqrt{C_A K'} \frac{L}{2} \sinh \sqrt{C_A K} a\right) \quad (25)$$

Where G is a function of the unknown spring constant K

With eq. 25

$$\frac{d\delta N_c}{dx} = \frac{C_B \delta P G}{C_A}$$

and thus

$$\delta \Delta_s = \frac{C_B \, \delta P G}{C_A \, K} \quad (26)$$

At any shear connector location X and for any load increment δP we have measured $\delta \Delta_s$. We now solve Eq. 26 for K by trial and error or graphically. This latter method is used here. The change in the shear connector force is then at this location x:

$$\delta F_c = \lambda K \, \delta \Delta_s \quad (27)$$

where λ is the connector spacing.

4.0 Description of Tests

4.1 Cantilever tests

4.1.1 C1a - After several load increments separation was noticed between the concrete and the compression chord at the last shear connector. Then a tension crack developed at the last shear connector and eventually extended nearly to the top of the slab. As the maximum load was obtained a load report was heard, which later inspection revealed was caused by the failure of the first three shear connectors. The loading was continued until the compression chord buckled.

The failure was attributed to yielding of the tension chord, followed by the failure of three of the shear connectors and then the buckling of the compression chord.

4.1.2 C1b - The load was applied to the cantilever in increments until a weld failed. The load was removed, the weld was repaired since no damage was done before the failure occurred.

The first cracks between the slab and compression chord were noticed as the load approached that making the tension chord yield. The next load increments resulted in the yielding of the tension chord and considerable separation of the slab and compression chord at the last shear connection. The compression chord at the last shear connector began to buckle, a loud report occurred, indicating the failure of the shear connectors.

The failure occurred due to the yielding of the tension chord, the buckling of the compression chord and then the failure of the shear connectors.

4.1.3 _C4 - With only a couple of load increments applied the slab at the first shear connector cracked nearly to the top due to the large rotation. As the next load increments were applied a separation occurred between the compression chord and the slab from the first to third shear connectors. With the next load increment the tension chord failed where it was welded to the connecting bolt.

The failure was due to the untimely failure of the tension chord connection.

4.1.4 _C7 - The load was applied and increased until the tension chord yielded at which time the slab at the last shear connector cracked to mid-depth. As the load was increased beyond this point a loud report was heard. Later inspection revealed that the first and second shear connectors had failed. More load was applied until the compression chord buckled.

The failure was attributed to the yielding of the tension chord, followed by the fracture of the two shear connectors and then the buckling of the compression chord.

4.1.5 _C8a - After the load had reached near the value causing yielding in the tension chord a crack at the first shear connector had developed a considerable way into the slab. The tension chord connection then failed. The load was removed, the tension connection was then repaired.

The load was applied until again near the yield point of the tension chord. A tension crack in the slab developed at the third shear connector. The application of load was continued until the tension chord again failed in the vicinity of the connection weld.

The failure was due to the fracture of the weld connection of the tension chord.

4.1.6 C8b - The load was incremented for some time before the first tension crack was observed at the first shear connector. The load was increased until cracks also developed at the third shear connector. This maximum load was then held for some time while the deflection increased. Finally the tension connection failed.

The failure was a result of the fracture of the tension chord connection.

4.1.7. C9 - After several load increments were applied a slight separation of the compression chord from the slab was noted. Additional loading resulted in the fracture of the tension chord. The load was removed and the tension chord was repaired.

The load was again applied until the stress in the tension chord was near the yield point at which time a load report was heard. Later investigation revealed that three of the four shear connectors had fractured. Additional load increments were applied until the compression chord buckled.

The failure was attributed to the fracture of the shear connectors followed by the buckling of the compression chord.

4.1.8 C10 - The load was applied in increments until considerable separation was noted between the compression chord and the slab. This occurred between the last shear connector and the support point of the cantilever. A tensile crack also appeared in the concrete at the first shear connector. Addition load increments resulted in the slab separation increasing considerably and the tensile crack extending almost to the top of the slab. The next load increments resulted in the buckling of the compression chord and the fracture of the shear connectors.

The failure of this cantilever was attributed to the buckling of the compression chord and then the fracture of the shear connectors.

4.2 Beam tests

4.2.1 B1 - The application of load was done in increments at which time readings and observations were made. The first cracks in the concrete slab occurred at the load points at a fairly high load. Increasing the load slightly caused a considerable separation of the slab from the compression chord in the vicinity of the second shear connector from the left. With additional load a loud report was heard and the left compression chord buckled laterally about one inch. The three shear connectors failed at the same time.

Failure was caused by the buckling of the compression chord followed by the fracture of the shear connectors.

4.2.2 B2 - The load was applied in increments until nearly the maximum value was obtained before any cracks were observed. The cracks occurred in each span at the load points and at each shear connector closest to the load points. With the application of the next load increment a loud report was heard. Examination of the beam indicated considerable separation at the last shear connector in the right span. On attempting to increase the load the compression chord at this last shear, buckled vertically.

The failure was due to the compression chord buckling followed by the fracture of the shear connector.

4.2.3 B3 - The load was applied in increments until half way to the maximum load before a slight separation of the compression chord and slab occurred. Additional loading increased the amount of separation until, at

the second extended web in the right span, cracks appeared in the concrete. At this time cracks also appeared around the third extended web of the right span. As the load was again increased the cracks around the second and third extended webs developed into general crushing of the concrete and finally with a loud report the compression chord at the third connector began to buckle. The extended webs then pulled out of the concrete.

The failure was attributed to the crushing of the concrete around the extended webs followed by the buckling of the compression chord.

4.2.4 B4 - The first cracks appeared in the concrete at the location of the first shear connector in each span after only a small load. Additional load resulted in cracks at the second shear connector and load point of each span. When more load increments were applied it became difficult to hold the load steady and then the first compression web member in the left span buckled.

The failure was caused by the buckling of the first compression web member in the left span.

4.2.5 B5 - The load was applied in increments as observations were made. Cracks developed in the slab at the first shear connector in each span. After another two load increments cracks had also developed at the load point and the previous two had extended further into the slab. With additional loading it became a little difficult to hold the load steady. As the load was increasing the second weld connection of the right span between the web member and bottom chord fractured.

The failure of this beam was a result of the weld failure of the web member to the tension chord.

4.2.6 _B6 - After several load increments a crack appeared at the first shear connector of the right span. With additional loading the compression chord began to separate from the slab and cracks appeared at the third shear connector in each span. After additional loading a crack appeared at the left load point. The next loading resulted in the fracture of a weld between web and the tension chord. The beam was unloaded and the weld repaired.

The beam was incrementally loaded to its previous value and the test continued. Shortly thereafter it appeared as if the tension chord had yielded as large deflections with small load increases were obtained. As more load was applied it was noticed that the concrete slab was being bent in the reverse direction as tension cracks were appearing on the top of the slab. As more deflection occurred the slab split just to the left of the left load point.

Failure was attributed to yielding of the tension chord followed by the splitting of the concrete.

4.2.7 _B7 - The load was applied in increments as observations were made. Cracks appeared around the third extended web of the left span and the compression chord separated from the slab between this point and the left load point. As more load was applied the cracks and separation increased. A loud report was heard but no evident damage could be seen. With more loading the one compression member at the third extended web began to separate considerably indicating the weld at this point had fractured. The loading then became difficult to hold steady as the separation and concrete cracks increased. The concrete cracks around the third extended web developed into general crushing. With a loud report the extended web pulled out of the concrete and the compression chord

buckled.

Failure was attributed to crushing of the concrete followed by the buckling of the compression chord.

4.3 Summary of Failures

4.3.1 Cantilever tests

C1a - yielding of tension chord, fracture of three shear connectors, buckling of compression chord.

C1b - yielding of tension chord, buckling of compression chord, fracture of the shear connectors.

C4 - failure of the tension chord connection.

C7 - yielding of tension chord, fracture of two shear connectors, buckling of compression chord.

C8a - failure of the tension chord connection.

C8b - failure of the tension chord connection.

C9 - fracture of three shear connectors, buckling of the compression chord.

C10 - buckling of the compression chord, fracture of the shear connectors.

4.3.2 Beam tests

B1 - buckling of the compression chord, fracture of the shear connectors.

B2 - buckling of the compression chord, fracture of the shear connectors.

B3 - crushing of concrete, buckling of the compression chord.

B4 - buckling of first compression web member.

B5 - failure of a weld between the web and tension chord.

B6 - yielding of the tension chord, splitting of the concrete.

B7 - crushing of concrete, buckling of the compression chord.

Table 1a - Cantilever Cross-Section Properties

Joist Type	C1a Hot Rolled	C1b Hot Rolled	C4 Cold Rolled	C7 Hot Rolled	C8a Cold Rolled	C8b Cold Rolled	C9 Hot Rolled	C10 Hot Rolled
Shear Connection	4 Studs	3 Studs	4 Studs	3 Studs	3 Studs	3 Studs	4 Studs	3 Studs
a (in)	84 3/4"	84 1/4"	89 1/4"	88"	85"	83 3/4"	85 1/4"	85"
de (in)	15.28"	15.28"	15.15"	15.28"	15.15"	15.15"	15.15"	14.97
Ast (in^2)	0.79	0.79	0.72	0.79	0.72	0.72	0.79	0.79
Asb (in^2)	0.54	0.54	0.52	0.54	0.52	0.52	1.09	1.09
Aw (in^2)	0.54	0.54	0.52	0.54	0.52	0.52	0.54	0.54
ys (in)	9.05	9.05	8.84	9.05	8.84	8.84	6.37	6.30
Is (in^4)	75.2	75.2	69.8	75.2	69.8	69.8	105.1	102.7
yr (in)	15.15	15.15	15.11	15.15	15.11	15.11	13.63	13.49
Ir (in^4)	144.2	144.2	133.7	144.2	133.7	133.7	254.0	248.5
Fy (Ksi)	50	50	50	50	50	50	50	50
f'c (psi)	6900	3380	6390	5825	4340	5710	3160	4060

Table 1b - Beam Cross-Section Properties

Joist Type	B1 Hot Rolled	B2 Hot Rolled	B3 Hot Rolled	B4 Hot Rolled	B5 Hot Rolled	B6 Hot Rolled	B7 Hot Rolled
Shear Connection	3 Studs	4 Studs	3 Extended Webs	3 Studs	3 Studs	6 Studs	3 Extended Webs
L (in)	186	186	158	186	186	186	158
a (in)	81	81	67	81	81	81	67
de (in)	15.15	15.15	13.00	15.45	15.45	15.15	13.00
Ast (in^2)	0.79	0.79	0.79	0.72	0.72	0.79	0.79
Asb (in^2)	1.09	1.09	1.44	1.07	1.07	1.09	1.44
Aw (in^2)	0.54	0.54	0.76C 0.57T	0.52	0.52	0.54	0.76C 0.57T
ys (in)	6.37	6.37	4.61	6.21	6.21	6.37	4.61
Is (in^4)	105.7	105.7	86.4	103.2	103.2	105.7	86.4
yr (in)	13.63	13.63	11.20	13.91	13.91	13.63	11.20
Ir (in^4)	254.0	254.0	241.0	259.7	259.7	254.0	241.0
Fy	50	50	50	50	50	50	50
f'c	3620	3860	2970	3120	3220	2050	2345

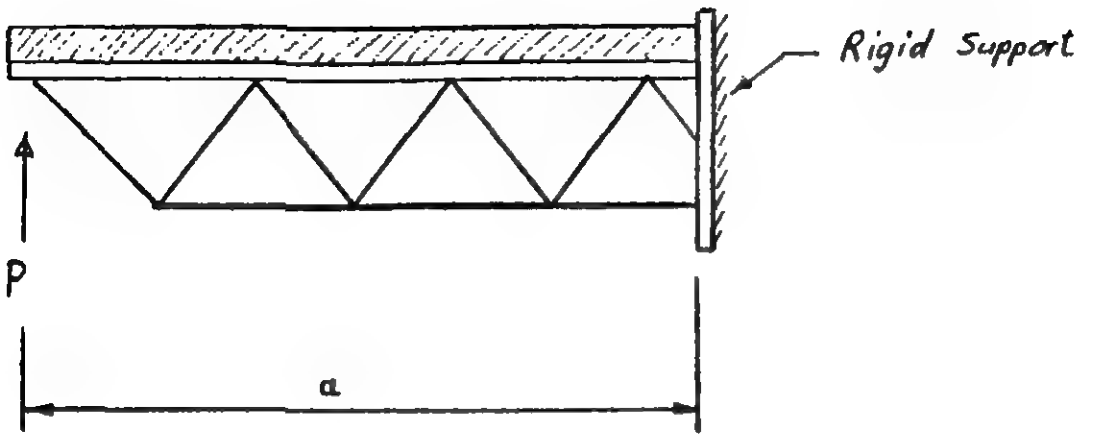

Fig. 1 Schematic View of Cantilever Tests

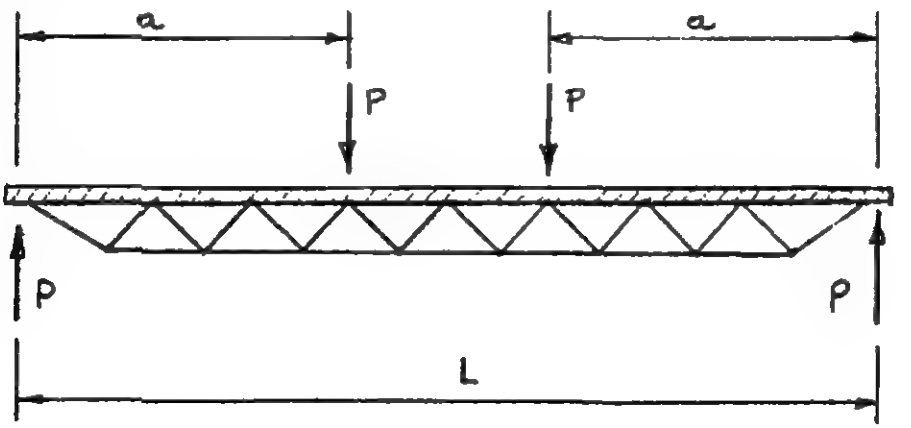

Fig. 2 Schematic View of Beam Tests

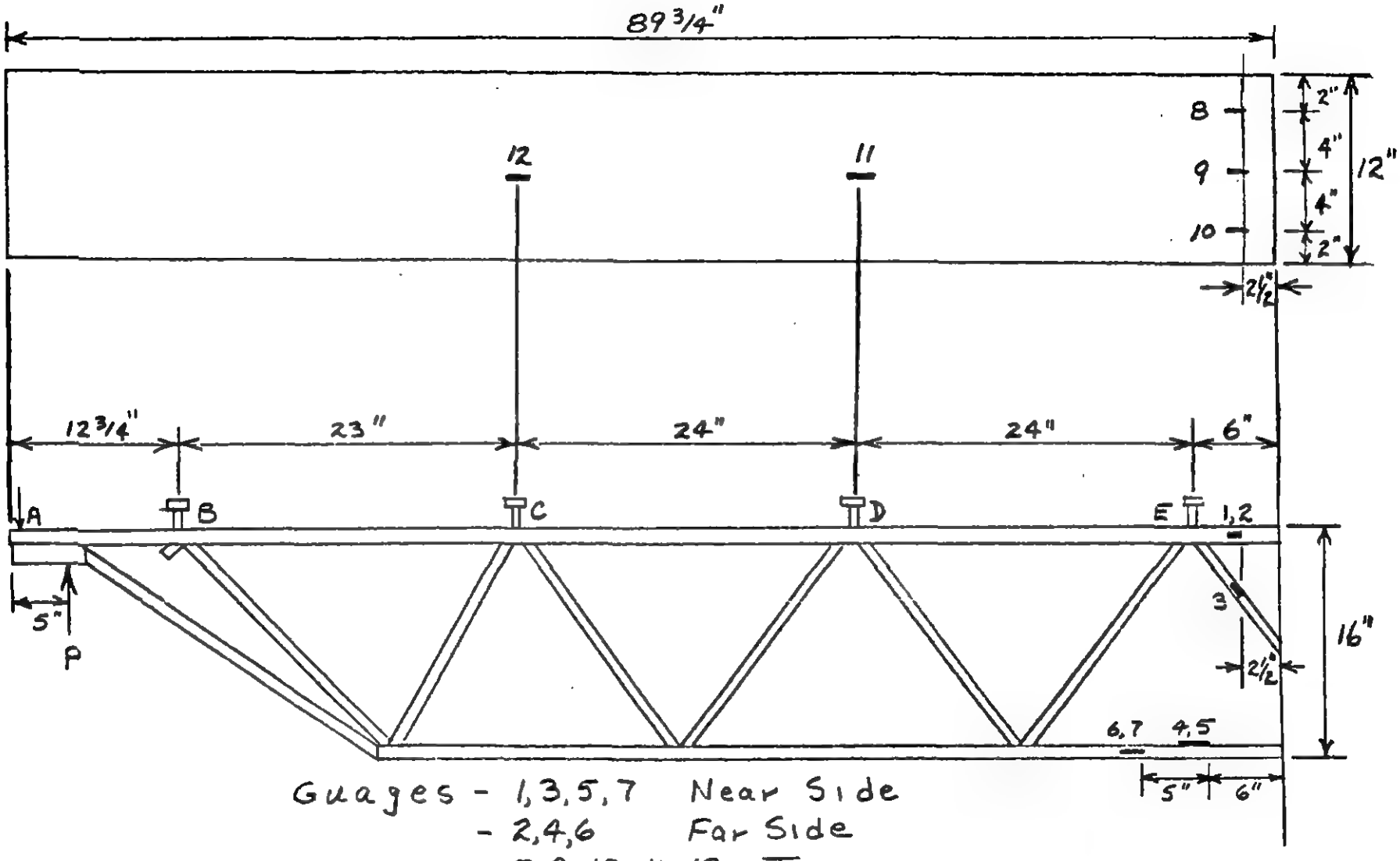

Guages - 1,3,5,7 Near Side
- 2,4,6 Far Side
- 8,9,10,11,12 Top

FIG 3a Test Joist C1a

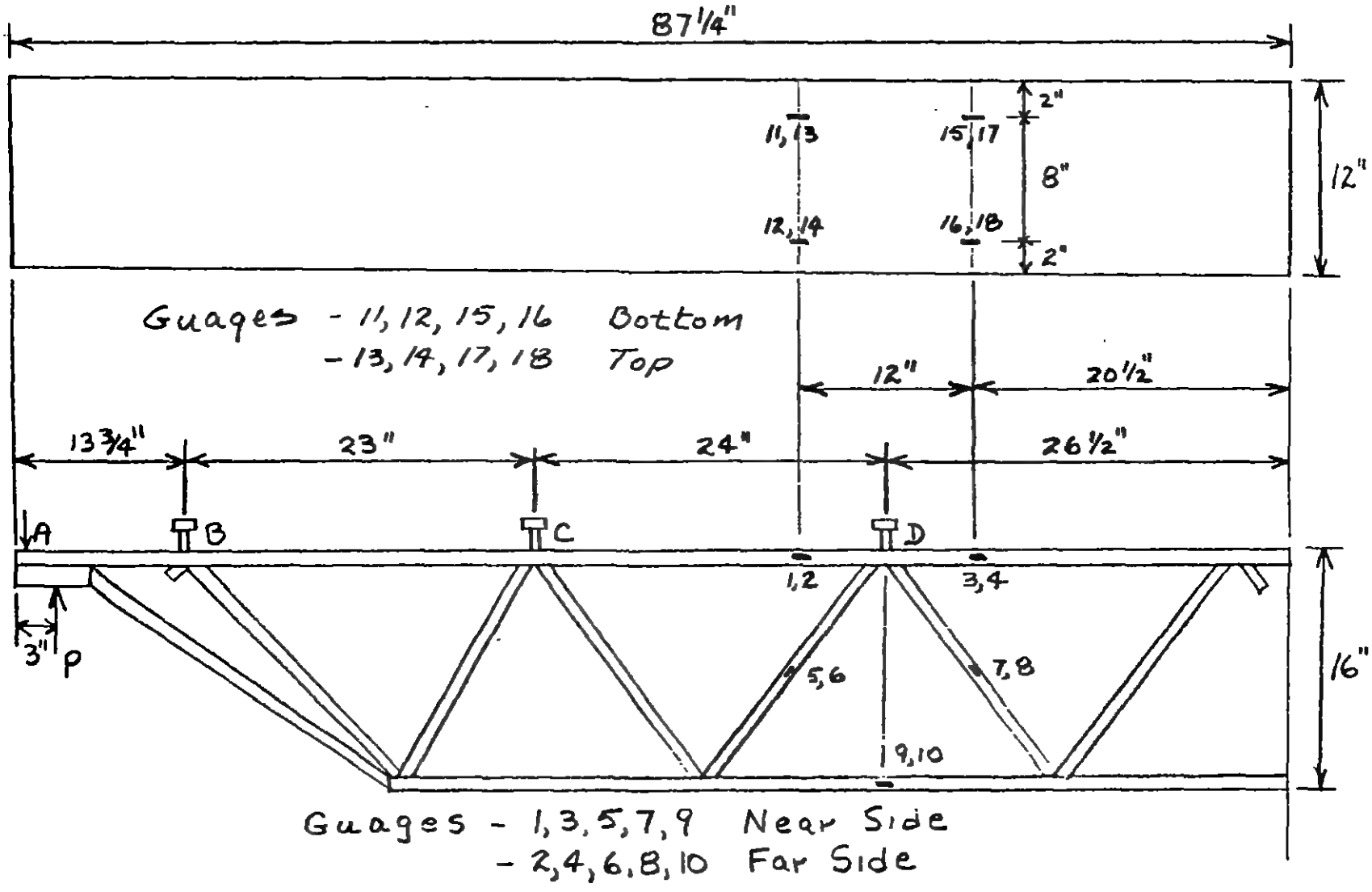

FIG 3b Test Joist C1b

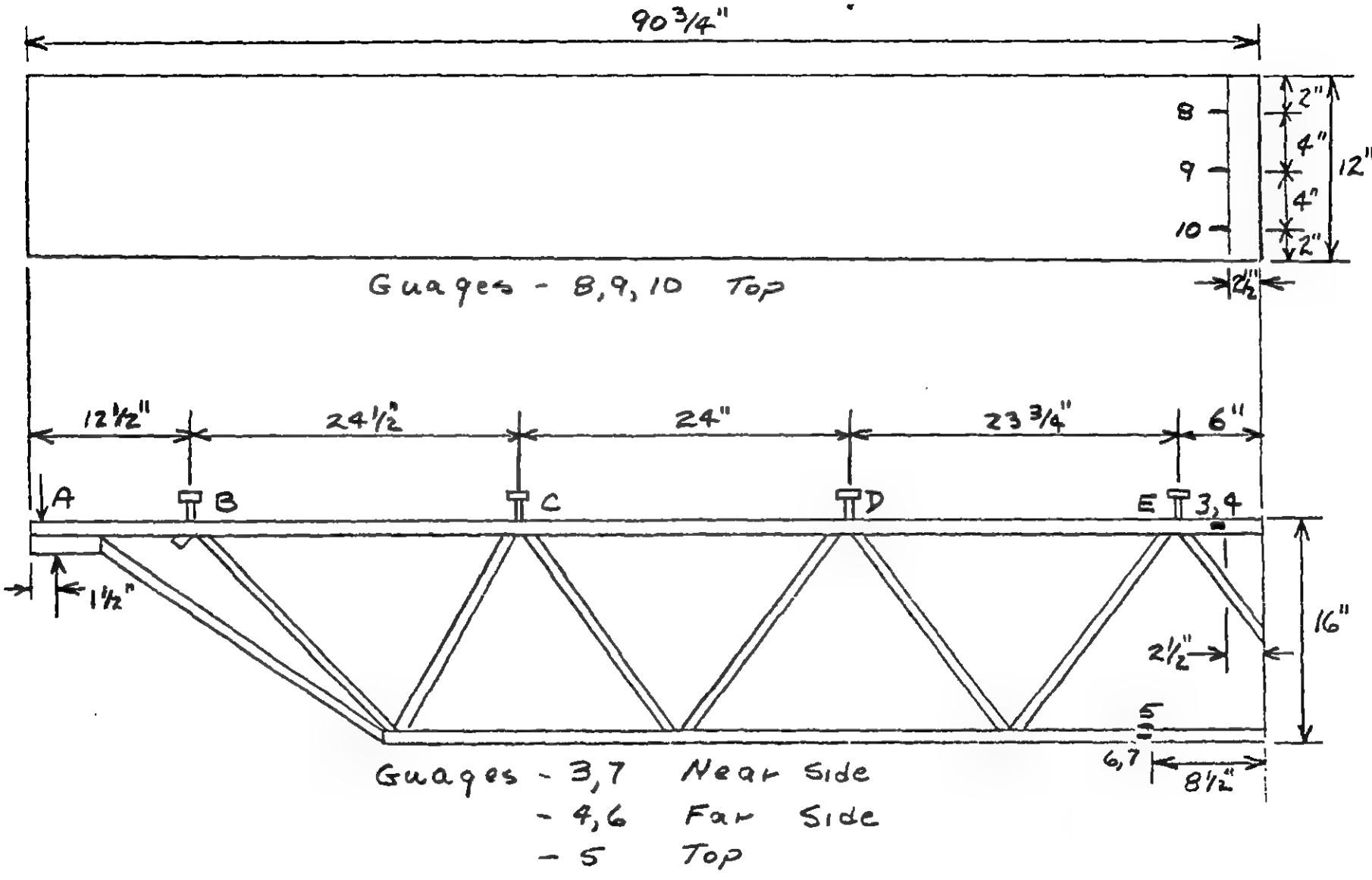

Fig. 3c Test Joist C4

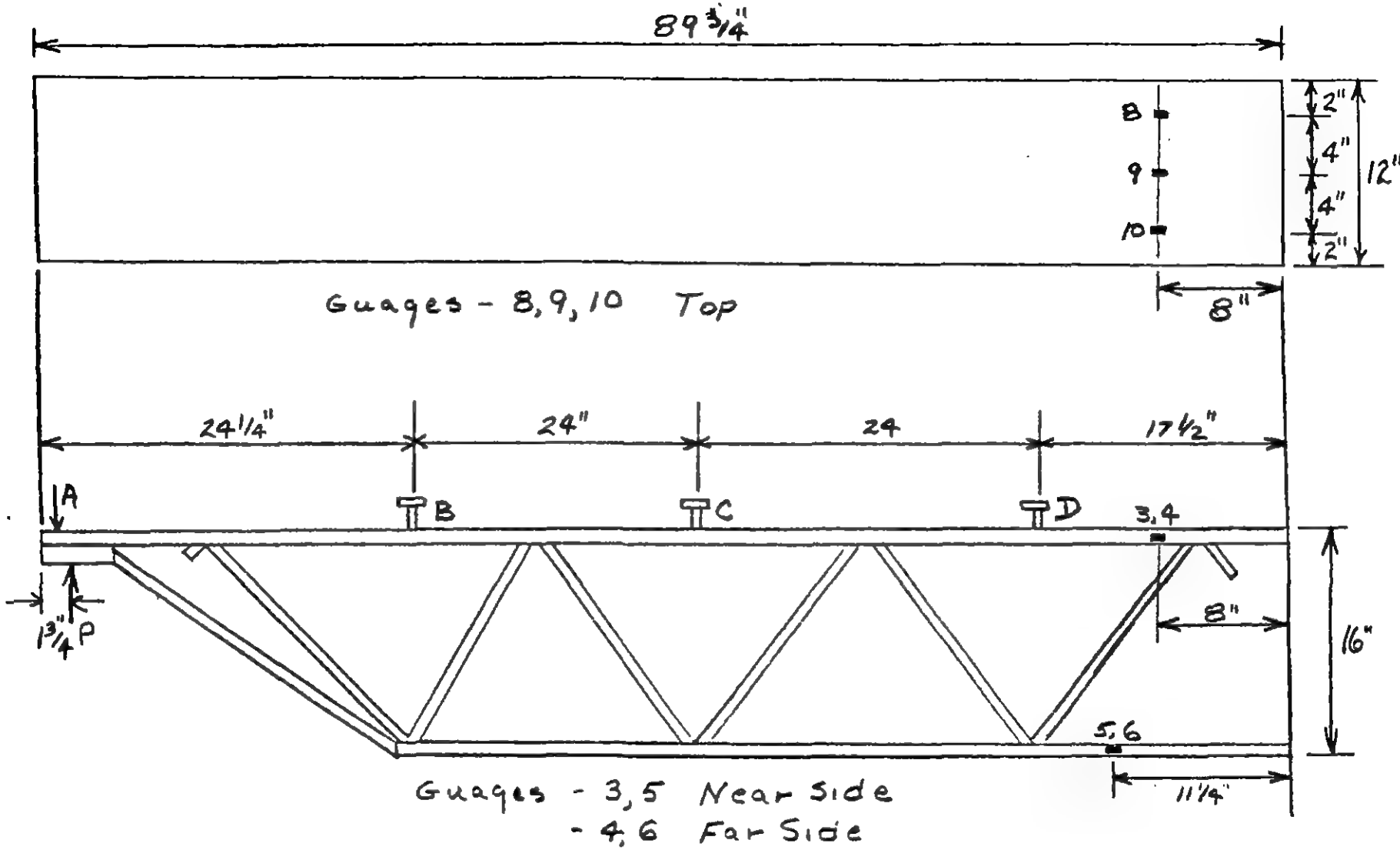

FIG. 3d Test Joist C7

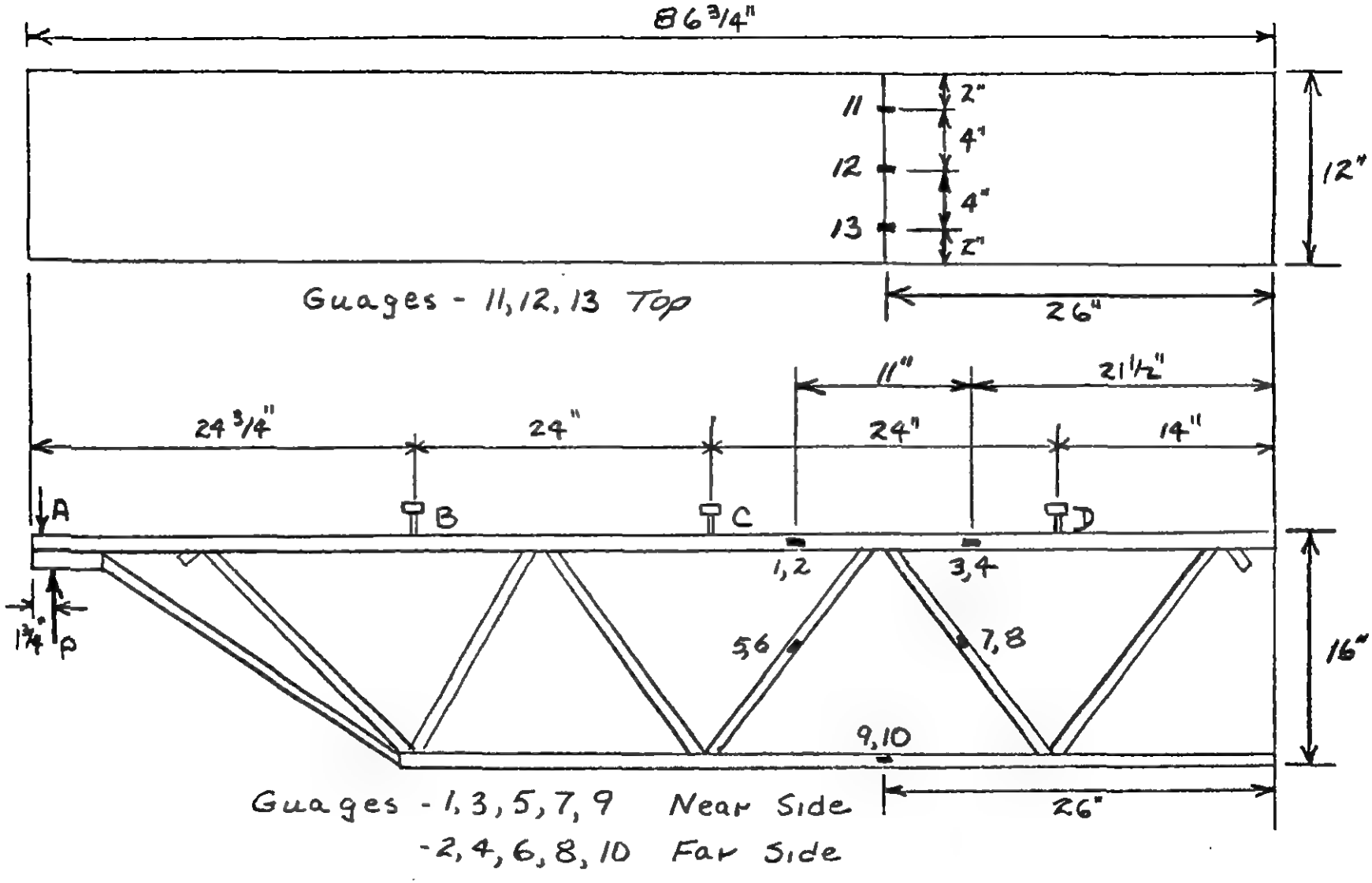

FIG 3e Test Joist C8a

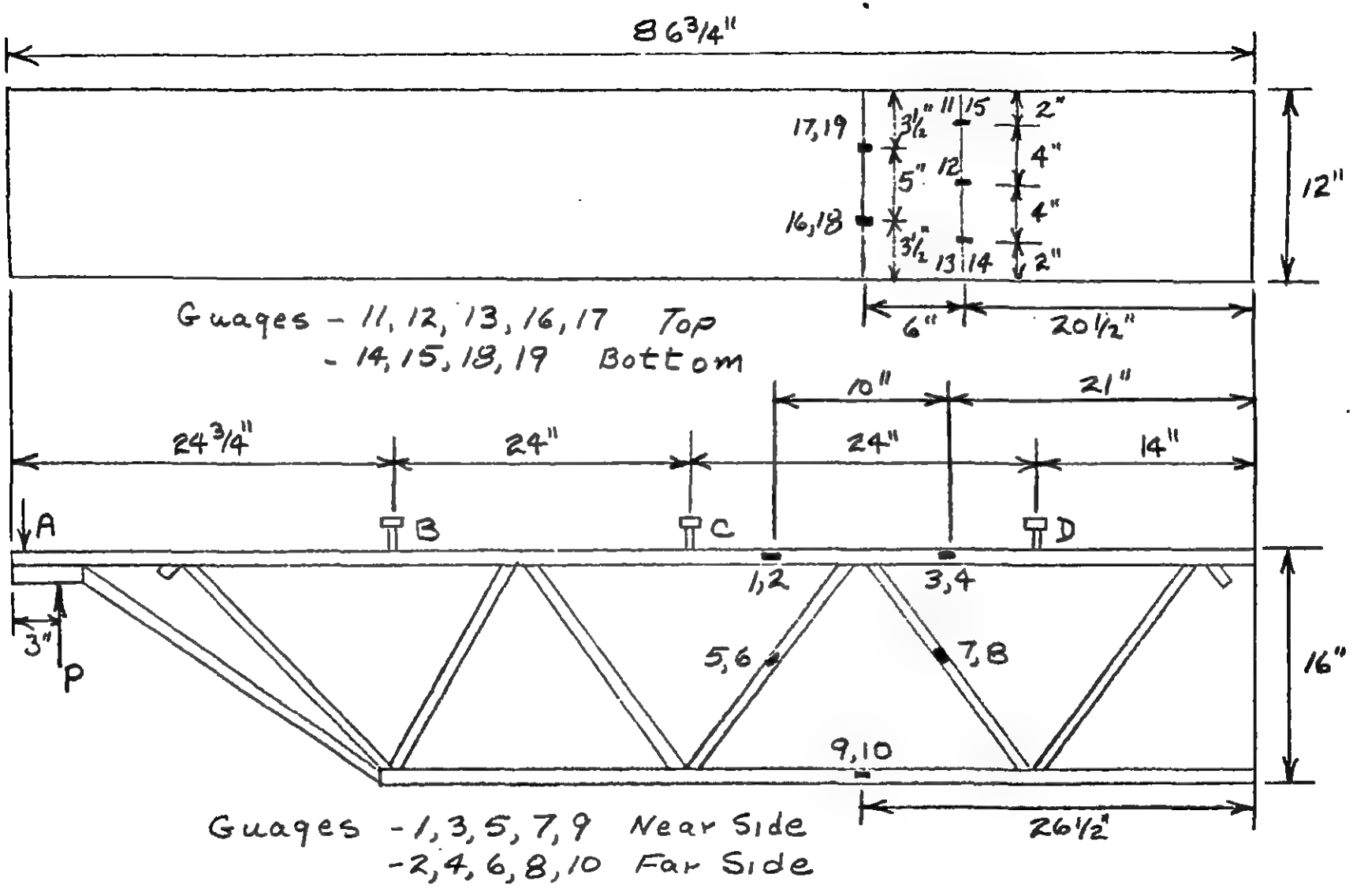

FIG 3f Test Joist C8b

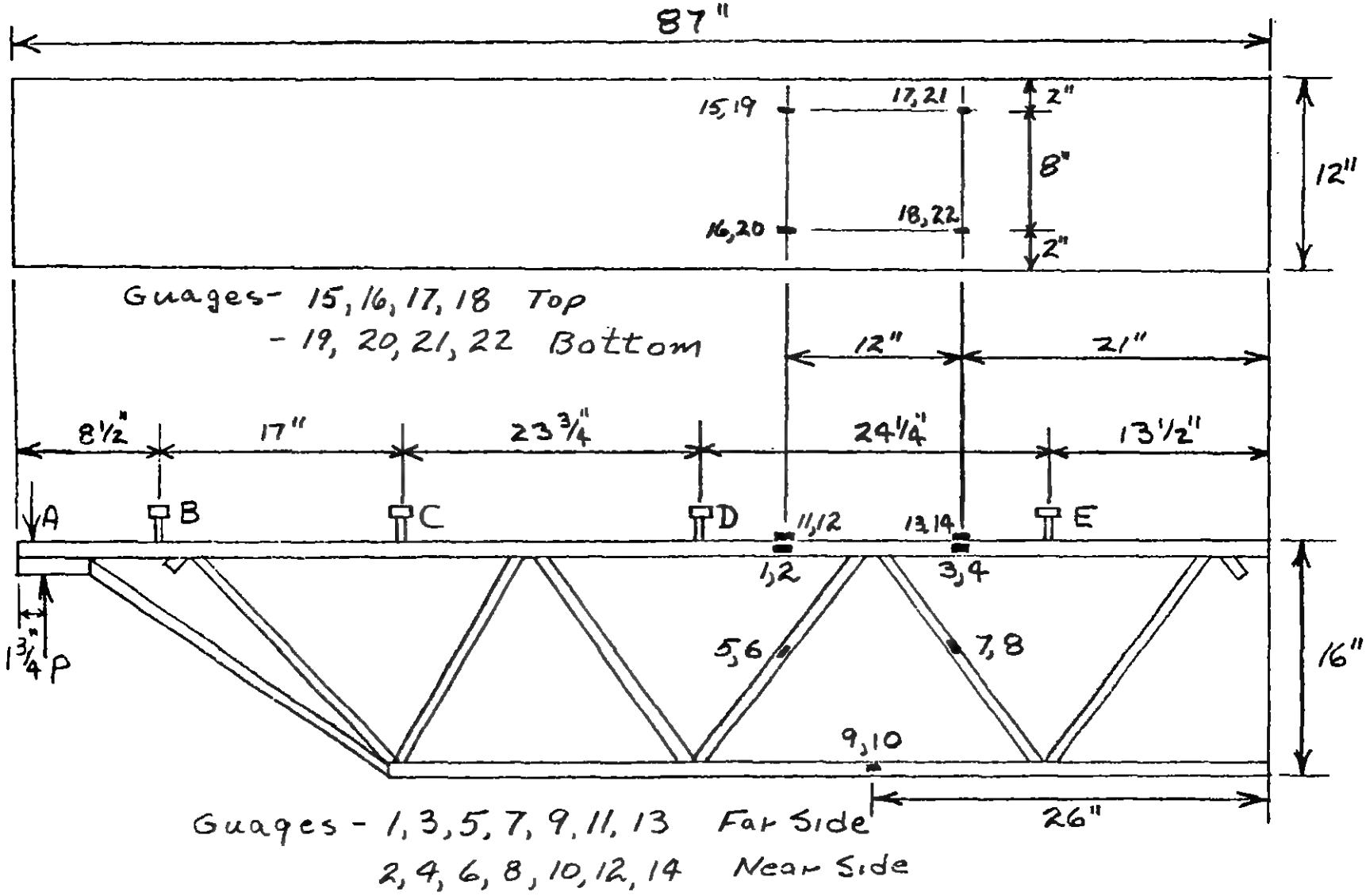

FIG 3g - Test Joist C9

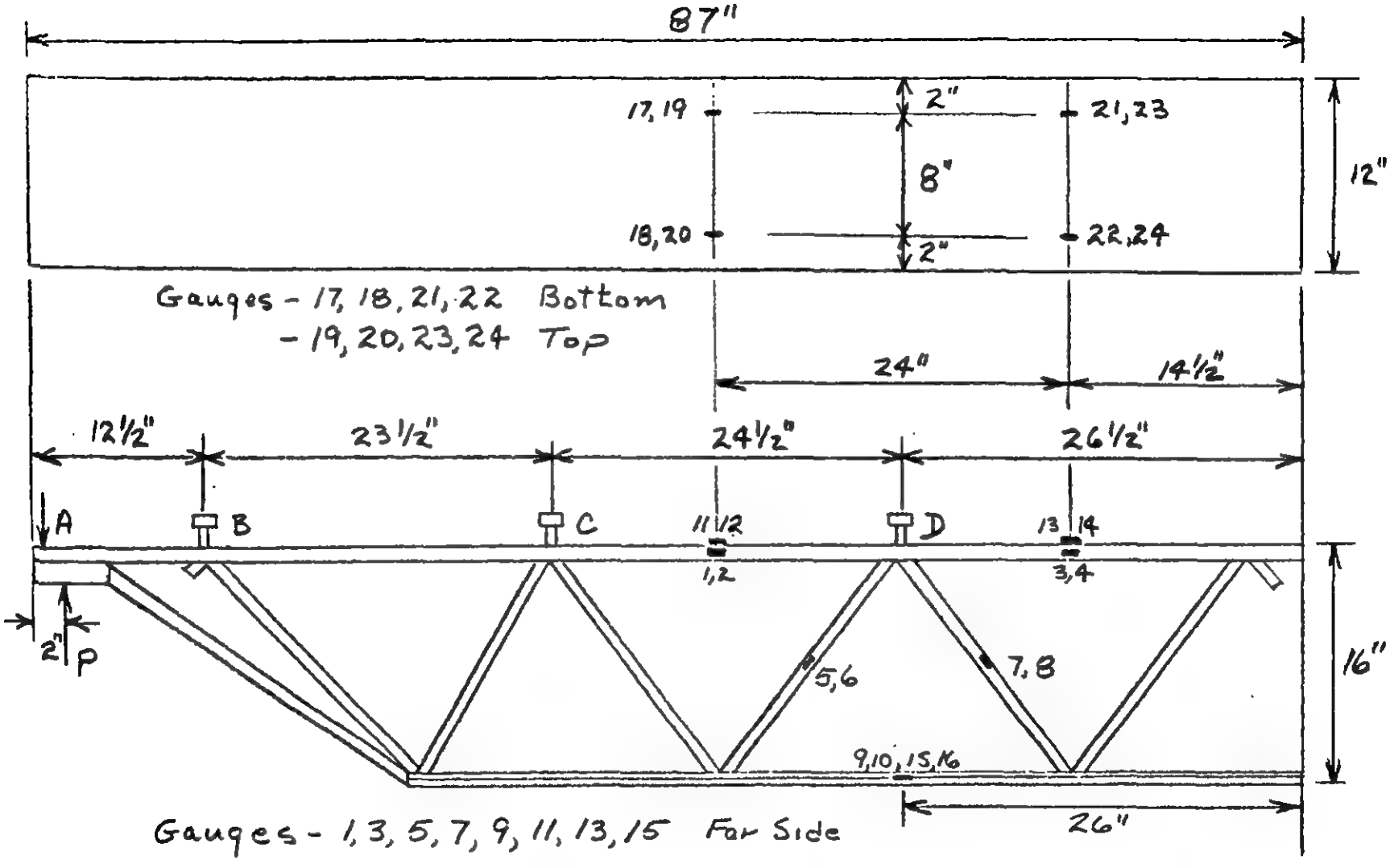

FIG 3 h - Test Joist C10

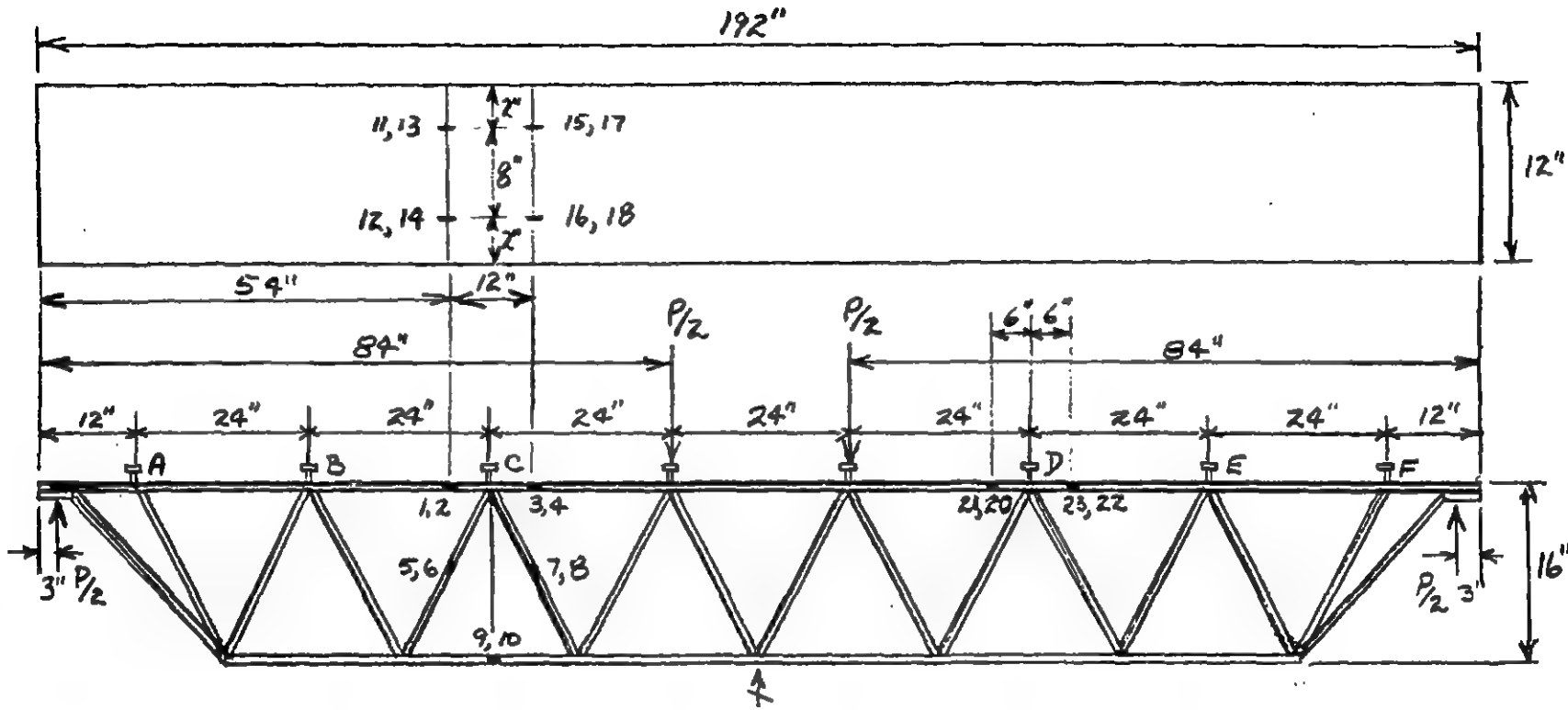

Guages - 1, 3, 5, 7, 9, 21, 23 Far Side
- 2, 4, 6, 8, 10, 20, 22 Near Side
- 11, 12, 15, 16 Bottom
- 13, 14, 17, 18 Top

FIG 3 i Test Joist B1

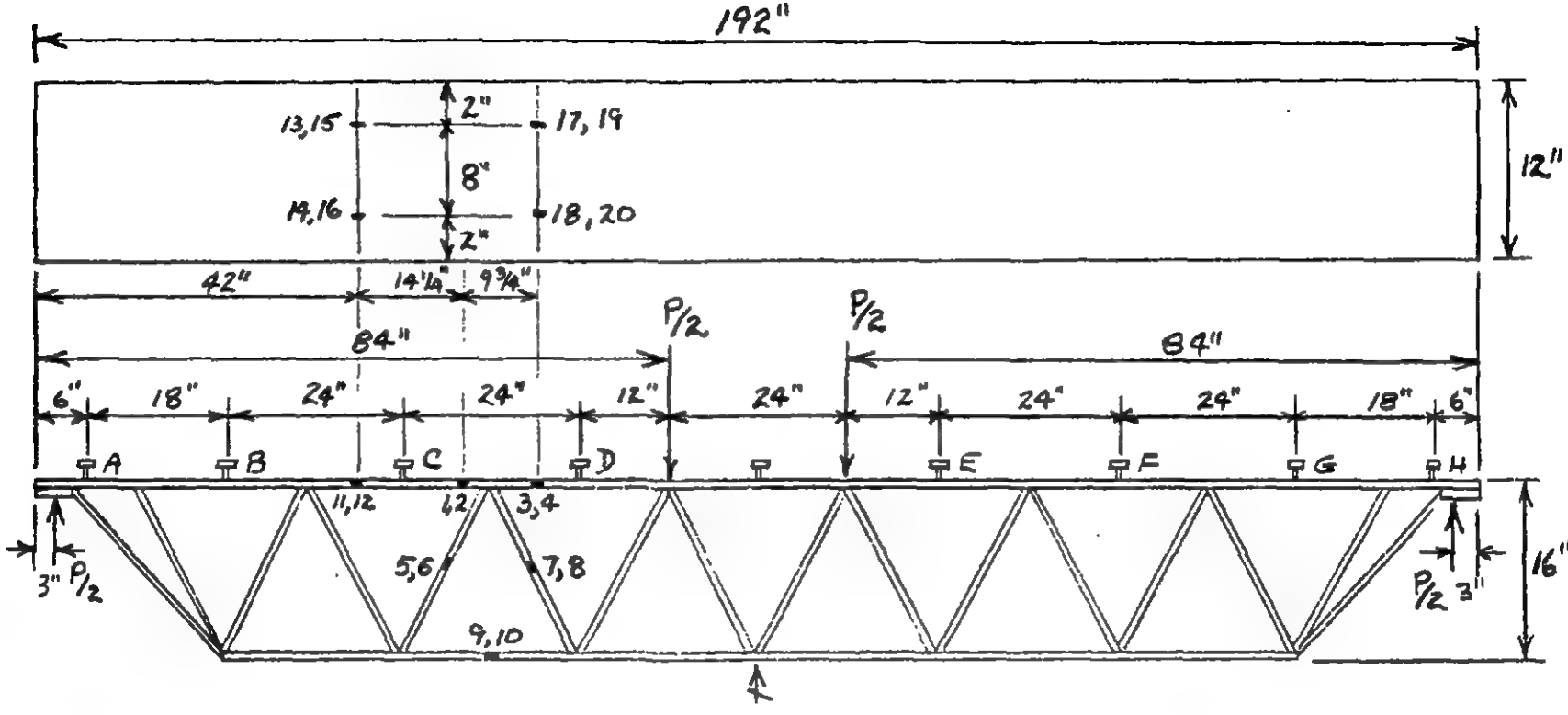

Guages - 1, 3, 5, 7, 9, 11 Far Side
- 2, 4, 6, 8, 10, 12 Near Side
- 13, 14, 17, 18 Bottom
- 15, 16, 19, 20 Top

FIG 3j Test Joist B2

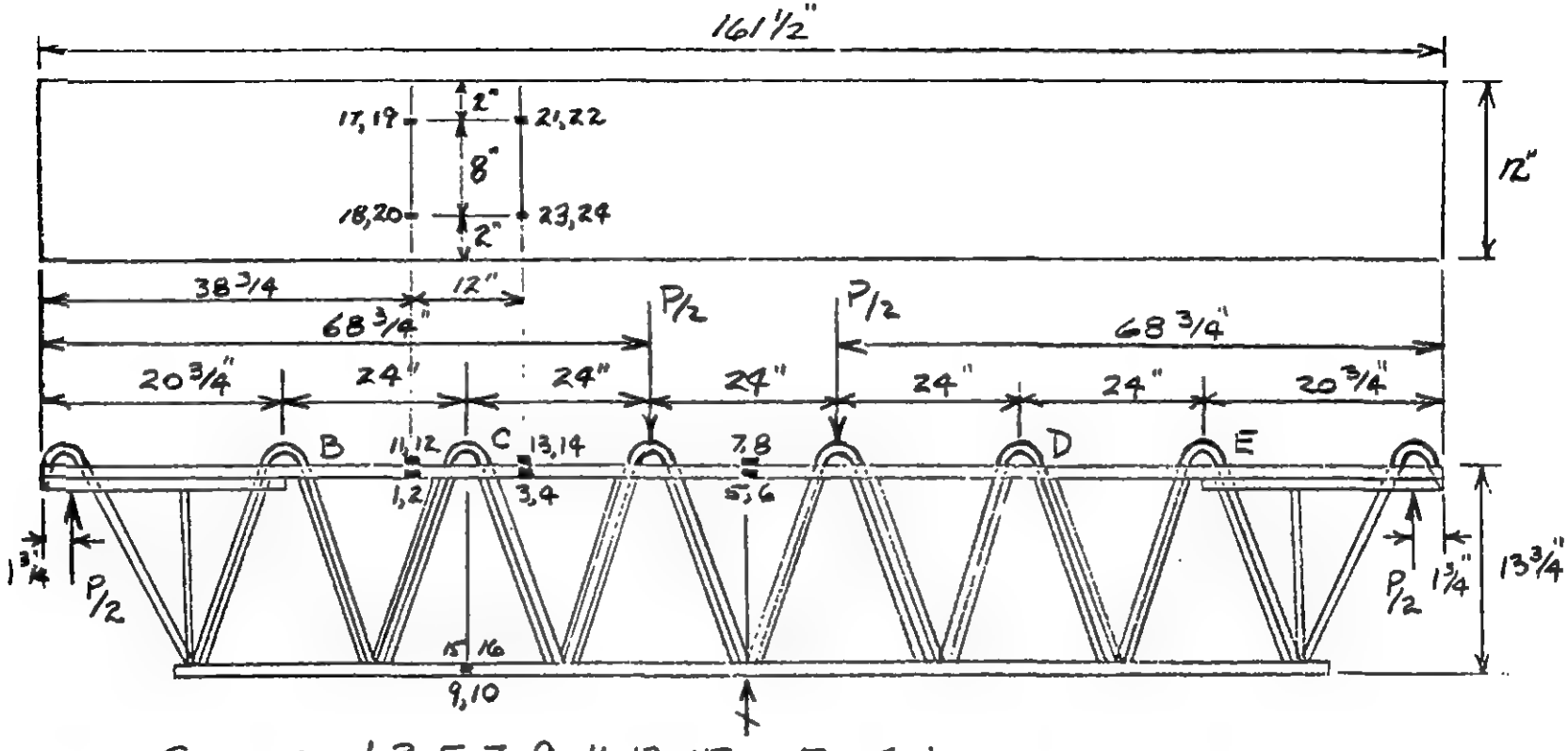

Guages - 1, 3, 5, 7, 9. 11, 13, 15 Far Side
- 2, 4, 6, 8, 10, 12, 14, 16 Near Side
- 17, 18, 21, 23 Bottom
- 19, 20, 22, 24 Top

FIG 3 k Test Joist B3

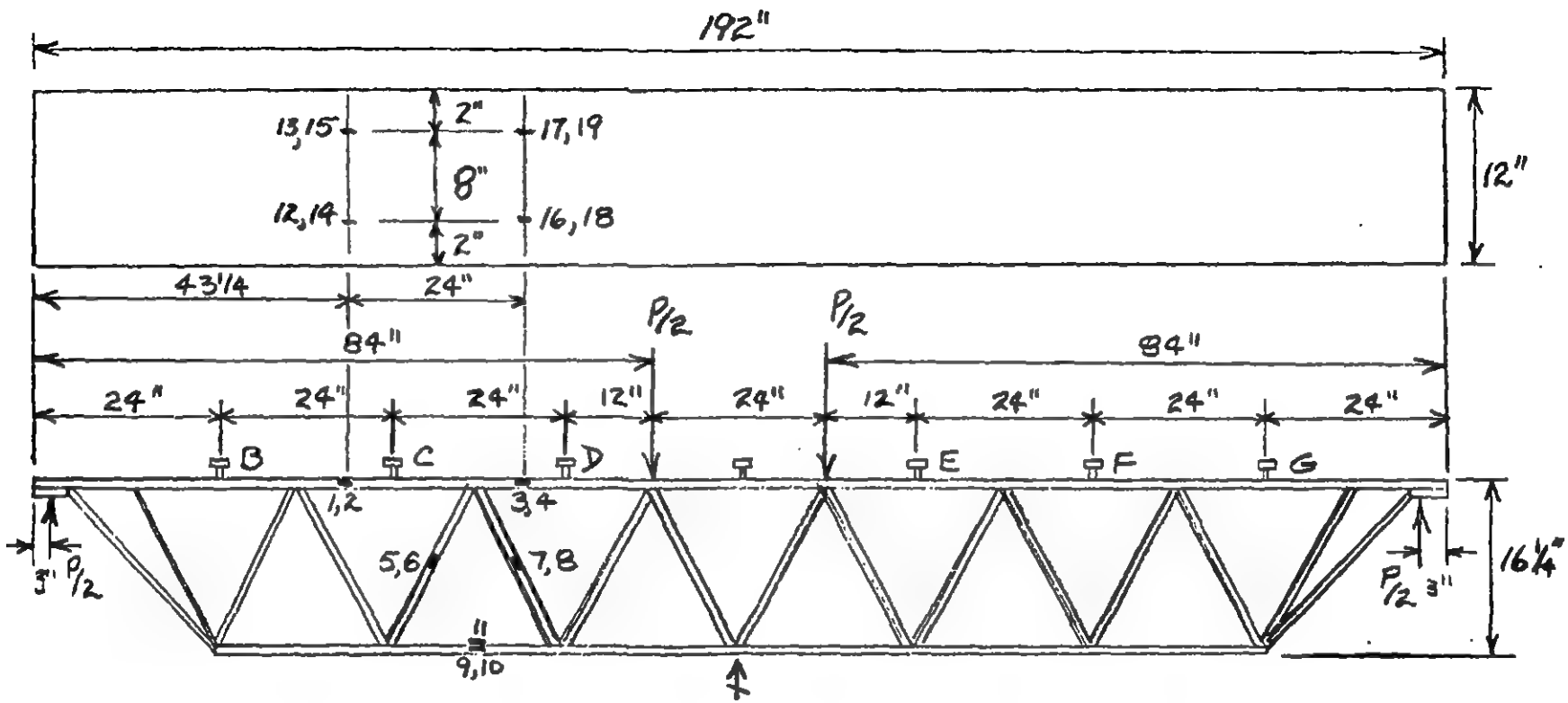

Guages - 1, 3, 5, 7, 9 Far Side
- 2, 4, 6, 8, 10 Near Side
- 11, Top of bottom chord
- 12, 13, 16, 17 Bottom
- 14, 15, 18, 19 Top

FIG 3 ℓ Test Joist B4

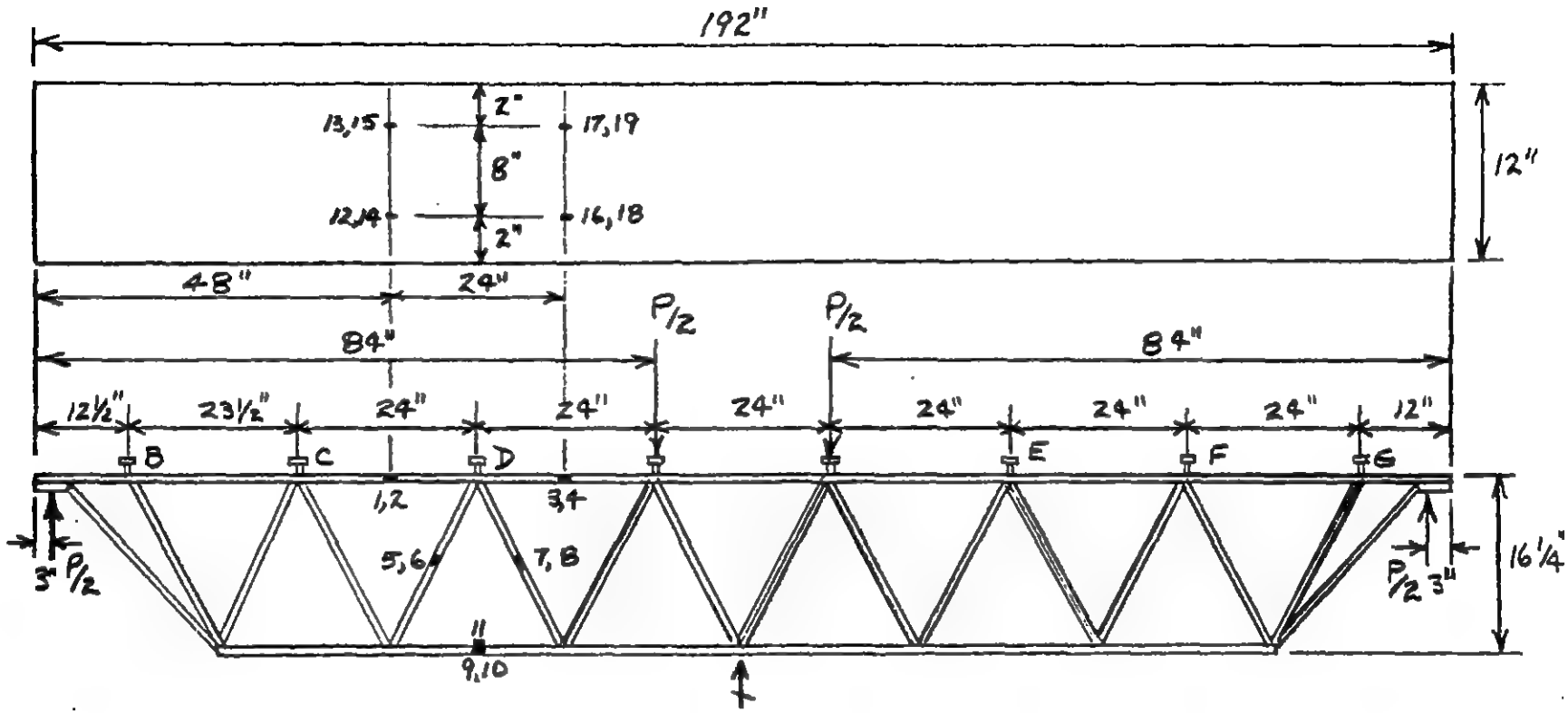

Guages - 1, 3, 5, 7, 9 Far Side
- 2, 4, 6, 8, 10 Near Side
- 11, Top of bottom chord
- 12, 13, 16, 17 Bottom
- 14, 15, 18, 19 Top

FIG 3m Test Joist B5

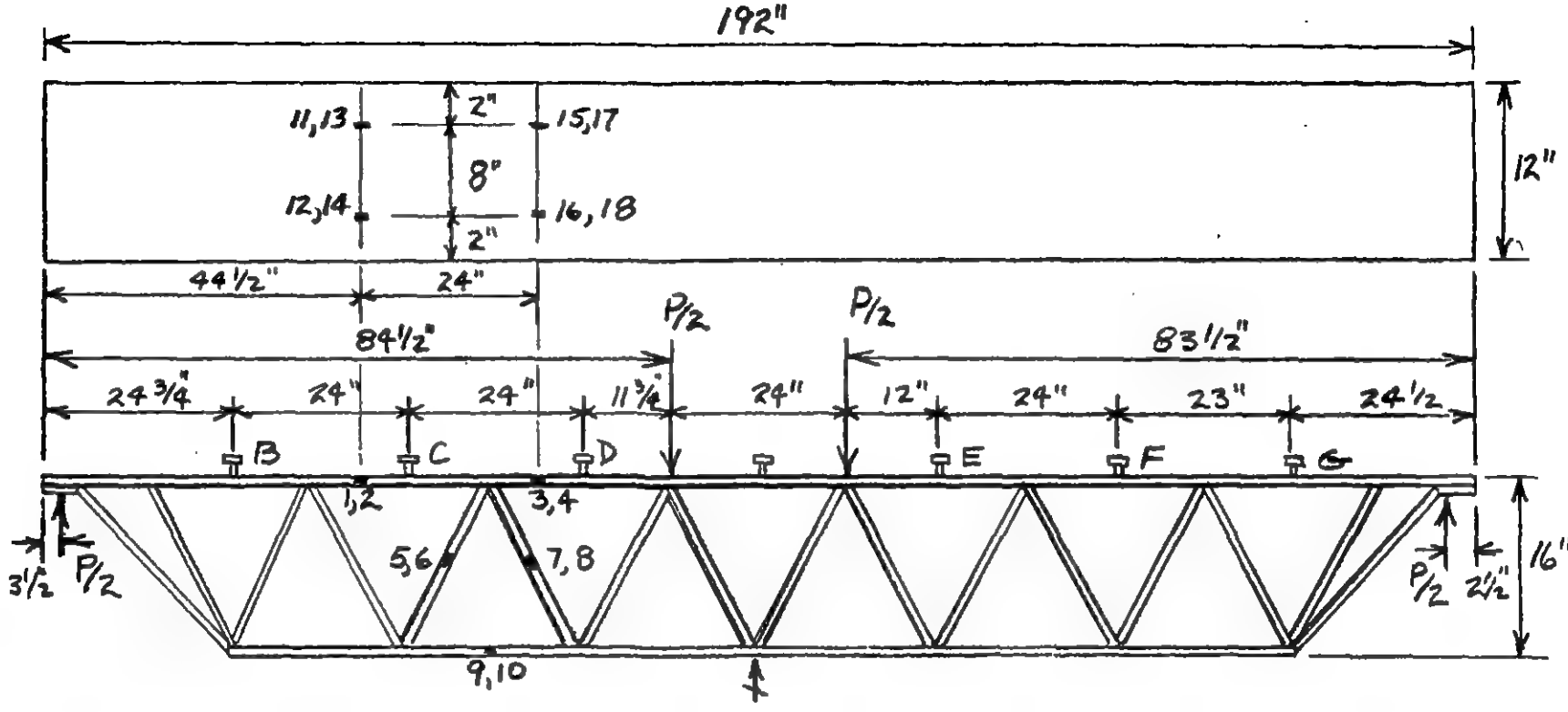

Guages - 1, 3, 5, 7, 9 Far Side
- 2, 4, 6, 8, 10 Near Side
- 11, 12, 15, 16 Bottom
- 13, 14, 17, 18 Top

FIG 3n Test Joist B6

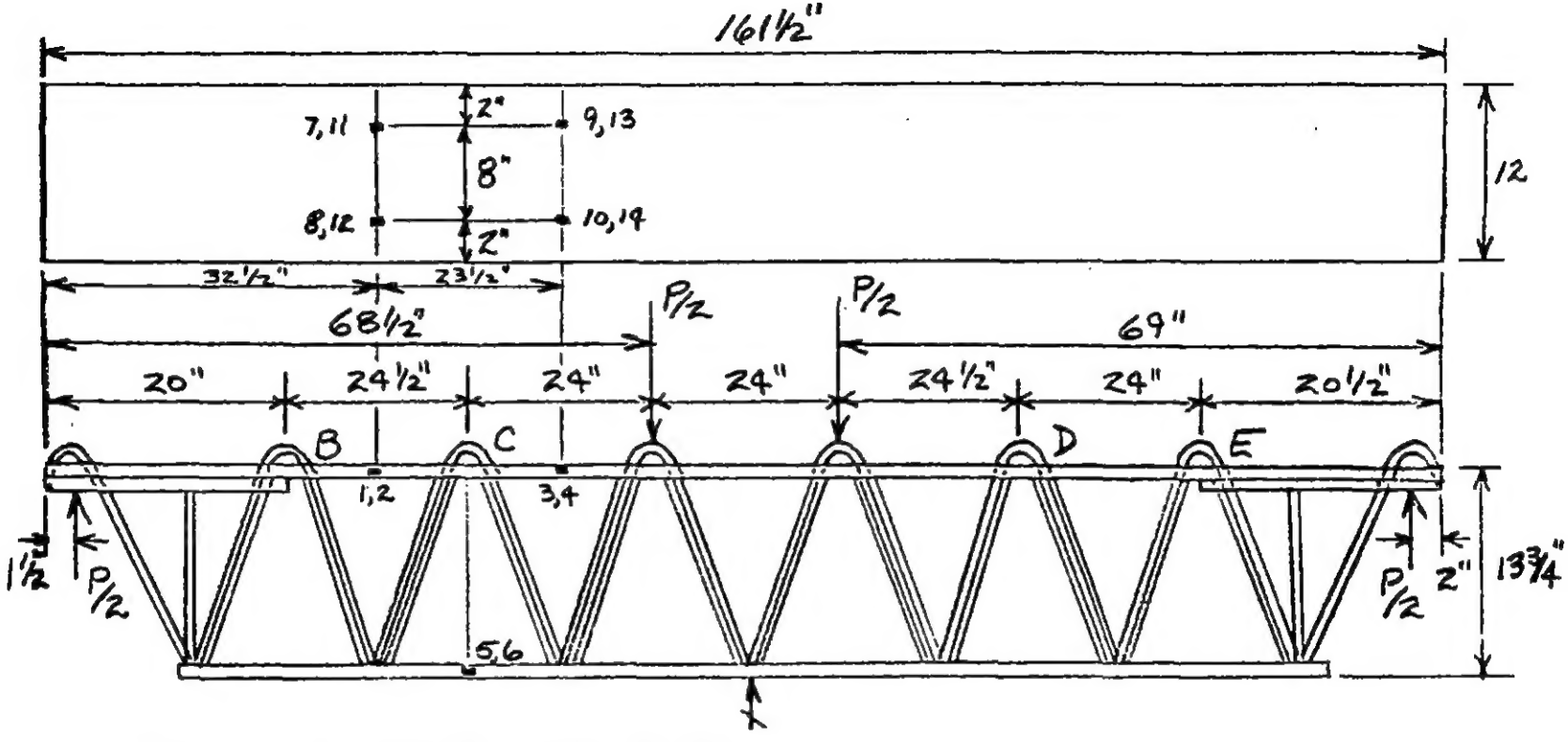

Guages - 1, 3, 5 Far Side
- 2, 4, 6 Near Side
- 7, 8, 9, 10 Bottom
- 11, 12, 13, 14 Top

FIG 30 Test Joist B7

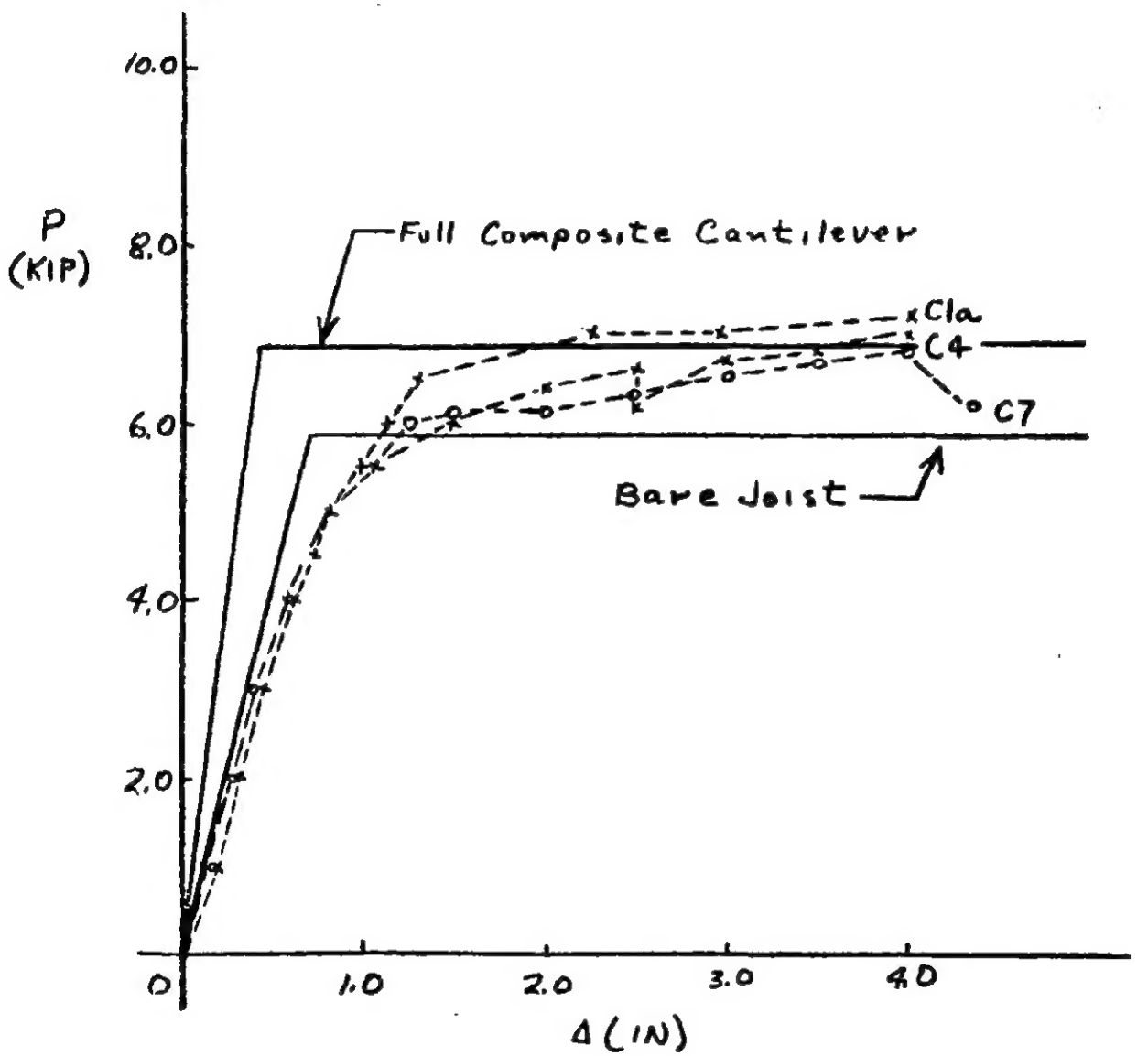

FIG 4a Load - Deflection Diagram for Cantilevers

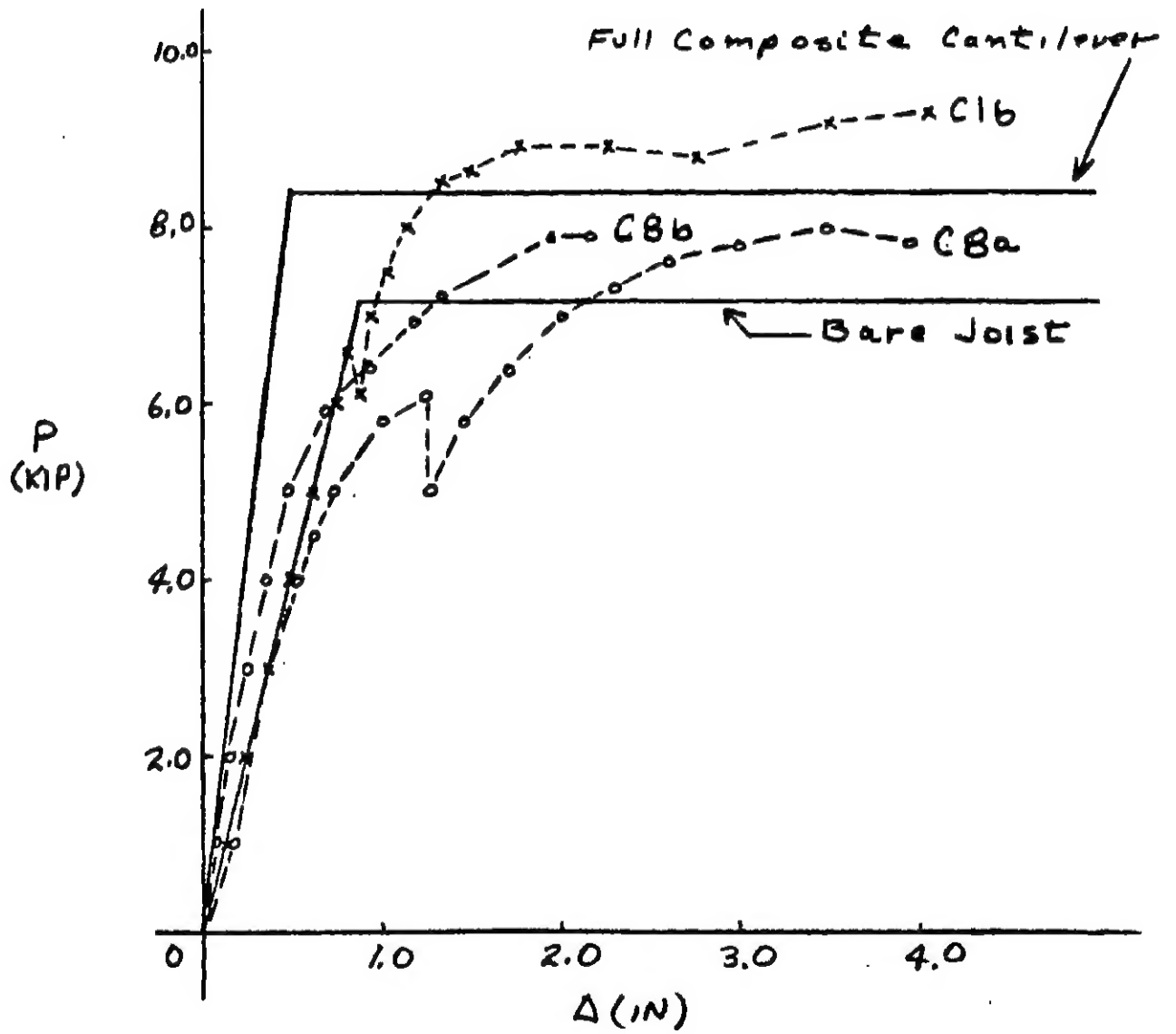

FIG 4b Load-Deflection Diagram for Cantilevers

ACW
SAVE

CC: F. E. Akin
H. F. Kilpatrick
A. C. Weber

October [illegible], 1[illegible]7

[illegible]. D. BAY

TESTS ON COMPOSITE JOISTS
WASHINGTON UNIVERSITY

At a meeting of the Steel Joist Institute Research Committee on October 1[illegible] at Washington University, the preliminary tests on composite joists performed by Dr. [illegible] and [illegible] will be discussed.

It is interesting to note in the report that test numbers [illegible] and B7 which had extended web shear members are the ones singled out to be acknowledged as composite elements while all the other types of joists with shear connectors were identified as being acknowledged "partially composite."

It is further interesting to note that in the recording of slip between slab and top chord the [illegible] joist which had extended web shear members of our type recorded deflections of one ten-thousandth of an inch while all others were recorded in hundredths and thousandths of inches. It is explained in the report that the small amount of movement between top chord and concrete slab necessitated changing the scale for deflection and slip readings.

It will be interesting to see the reaction of the rest of the Steel Industry to these tests, and we should know rather shortly whether we are to continue on composite joist construction on our own rather than wait for the Steel Joist Industry to give up and develop something that we could also use.

The test reports as shown bear out the comments that we have heard from the faculty at the Engineering School that only our type of joists acted compositely, and in no case at normal design loads were there ever any stresses recorded in the top chord of the Laclede type joist.

A. C. Weber

ACW:pjz